https://doi.org/10.5194/wes-2024-66
Preprint. Discussion started: 10 June 2024

Dynamic Response of Offshore Wind Turbine Structure under Multi-load Coupling Based on DEM and FEM Joint Analysis

Xin GUAN[1*], Haoran XU[1], Ying YUAN[2], Shuaijie WANG[1], Chenhao ZHAO[1], Hua YU[1]

1 School of New Energy, Shenyang Institute of Technology, Shenyang 110136, China;
2 China Quality Certification Center, Beijing FengTai 100000
**Corresponding author Email: xin_guan@sina.com*

Abstract: The structural dynamic characteristics of offshore wind turbines are directly related to the operational safety and equipment reliability of these turbines in service. However, due to the complex working conditions, a single load analysis fails to accurately reflect the structural dynamic characteristics during actual operation. In this study, we focus on the 5MW offshore wind turbines and establish a three-dimensional turbulent flow field model at sea using the Kaimal wind speed spectrum. Additionally, we incorporate the Kärnä ice force spectrum to develop a mathematical model for floating ice. By combining multiple working conditions through permutation and combination techniques, we replicate the actual operating environment of offshore wind turbines. Leveraging OpenFAST's open computing capabilities and EDEM's discrete element analysis method, we investigate the dynamic response characteristics of wind turbines under separate and coupled effects of wind load, wave load, and ice load across different offshore working conditions. Our findings indicate that under coupling effects from wind-wave-ice loads, lateral and longitudinal displacement at the tower top as well as lateral and longitudinal bending moment at the tower foundation are greater compared to individual loads; however, cumulative fatigue damage caused by coupling loads on wind turbines is less than that resulting from individual loads.

Keywords: Offshore wind turbine, wind-wave-ice load, coupling, dynamic response

0 Introduction

In recent years, China has witnessed the extensive construction of offshore wind farms. The safe running of offshore wind turbines in the northern sea is affected by intermittent floating ice and turbulent winds, which are unique working conditions they must confront. The intermittent impact of floating ice presents a distinctive marine environment challenge for offshore wind power development, as it induces long-lasting and relatively stable vibrations on the overall structure due to ice load coupled with ocean current movement (LIU Weimin et al., 2019 and ZHANG Dayong et al., 2018). Such vibrations can lead to fatigue damage and continuous structural strain accumulation under sustained exposure to ice load. Additionally, the wind load exerts significant vibrational effects on both the tower foundation and mud surface line position of the unit's platform structure. These loads and their coupling effects alter aeroelasticity and structural dynamic response of wind turbines, making it crucial to investigate their influence on operational status under different marine environmental conditions. Considering various installed capacities and structural types of wind turbines nowadays, it becomes evident that annual ice formation characteristics in the northern Gulf of China pose a substantial threat to operational safety in this region (HUANG Yan et al., 2016). Therefore, studying wind load, ice load, wave load along with their interactions holds great engineering significance for advancing offshore wind power development in China.

Shi Wei et al. (2021) employed ANSYS/AQWA to establish a hydrodynamic numerical model for a semi-submersible floating foundation and conducted dynamic response analysis of a 10 MW offshore floating wind

https://doi.org/10.5194/wes-2024-66
Preprint. Discussion started: 10 June 2024

turbine under the influence of wind and waves. Hu Xuan et al. (2019) developed the Kane multi-body dynamic model for wind turbines, utilized the asynchronous Matlock model to simulate ice-induced vibration, and investigated the tower's dynamic response to turbulent wind loads and asynchronous ice-induced vibrations.

Yang Dongbao et al. (2021) employed a discrete element model with bond-crushing capability to characterize the damage and failure behavior of level sea ice, while utilizing the DEM-FEM coupling approach to simulate the interaction process between single-pile wind turbines and level ice under varying ice velocities and thicknesses. Wang Guojun et al. (2022) conducted a statistical analysis on the relationship between sea ice fracture length and sea ice thickness, and utilized a modified deterministic ice force function to calculate the structural response of the ice under measured conditions. Huang Yan et al. (2016) simulated the dynamic characteristics of wind power structures with significant differences in their master-slave structure, and performed transient dynamic analysis throughout the entire time domain. Zhang Lixian et al. (2019) carried out dynamic response analysis on single-pile offshore wind turbines subjected to floating ice using FAST coupling numerical analysis. Ba Yueqiao (2019) conducted fatigue analysis on offshore wind turbines in icy areas, and proposed a discrete element analysis method for determining ice loads on offshore wind turbines.

Based on ABAQUS finite element numerical analysis software and FAST numerical analysis software, Heinonen et al. (2008) conducted a dynamic characteristic analysis of single-pile wind turbines under the action of floating ice. The results showed that joint mathematical model analysis could improve the reliability of offshore wind turbine structural design. Wang et al. (2015) analyzed the fatigue characteristics influencing factors (ice load and wind load) of offshore wind turbines using Kärnä ice force spectrum model; Wei Shi et al. (2016) combined with semi-empirical structural action model of sea ice to analyze the dynamic response of single-pile wind turbine structures under different ice velocities and thicknesses' actions by ice cones. Matlock et al. (1971) added spring damping during loading process modeling analysis for floating ice, while Kärnä et al. (1999) proposed self-excited vibration response calculation method for marine structures based on actual measurement data from sea ice, which was calculated with sawtooth-shaped ice force function.

Currently, there is a limited number of studies investigating the impact of multi-load and ice load coupling on the fatigue life and safe running of offshore wind turbines. Considering the presence of floating ice in the northern seas of China and the national economic development's demand for offshore wind power, it is imperative to examine the dynamic response of offshore wind turbines under the combined influence of multi-load and ice load. In this study, numerical analysis using discrete element method and turbulent spatial coherence model was conducted to investigate the dynamic response of NREL 5 MW offshore wind turbines subjected to wind-wave-ice load coupling. The effects of different durations, ice excitation, and coupled load excitation on ultimate dynamic response and fatigue life were explored. Additionally, frequency domain response analysis was performed for large-scale offshore wind turbines under single action from ice load as well as coupled excitation from multiple loads. Cumulative effect on structural fatigue response due to various combinations of fatigue damage was

https://doi.org/10.5194/wes-2024-66
Preprint. Discussion started: 10 June 2024

considered, while relative errors in fatigue loading caused by individual actions (wind-wave-ice) versus coupling effects were calculated. These findings aim to provide valuable insights for future construction projects involving offshore wind power in cold regions within China.

1 Load Calculation

1.1 Calculation Theory of OpenFAST Wind Load

The aerodynamic load calculation of wind turbines primarily relies on the blade element momentum theory and the generalized dynamic inflow theory to accurately describe wind loads. In this study, we employ the blade element momentum theory to discretize wind turbine blades during load calculations. By iteratively calculating stress and moment acting on each blade element along the span, a closed-loop solution is established between lift and resistance coefficients and the induction factor. This approach ensures both engineering applicability and calculation accuracy.

(1) Kaimal turbulent wind spectrum model

The turbulent wind spectrum mathematical model is established using the Sandia method in TurbSim (VERITAS D N, 2010), and is generated based on the time series of Kaimal wind spectrum (IEC 61400-1, 2005) . The longitudinal (*u*), lateral (*v*), and vertical (*w*) directions of the fluid domain are defined with respect to the tower top coordinate system of the wind turbine, as illustrated in Figure 1

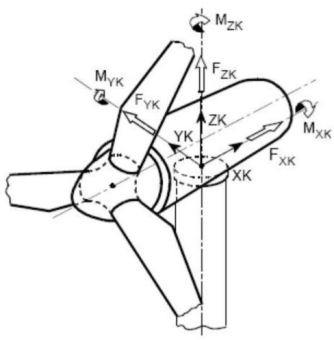

Fig. 1 Coordinate system at the top of the wind turbine tower

The mathematical formulation of the fluctuating wind velocity spectrum is presented.

$$S_K(f)=\frac{4\sigma_K^2 L_K/\bar{u}_{hub}}{\left(1+6fL_K/\bar{u}_{hub}\right)^{\frac{5}{3}}} \tag{1}$$

Where, K represents the directions of the fluid domain, namely *u*, *v*, and *w*; *f* denotes the circulation frequency; L_K is defined as the integral scale parameter.

https://doi.org/10.5194/wes-2024-66
Preprint. Discussion started: 10 June 2024

$$L_K = \begin{cases} 8.10\Lambda_U, & K = u \\ 2.70\Lambda_U, & K = v \\ 0.66\Lambda_U, & K = w \end{cases}$$

, Λ_U is turbulence scale parameter, Λ_U =0.7min(60m, HubHt), HubHt is the hub height. The standard deviation of different directions is defined as: $\sigma_v = 0.8\sigma_u$, $\sigma_w = 10.5\sigma_u$, and the turbulent wind load spectrum at the wheel hub of the wind turbine is formed, as shown in Figure 2.

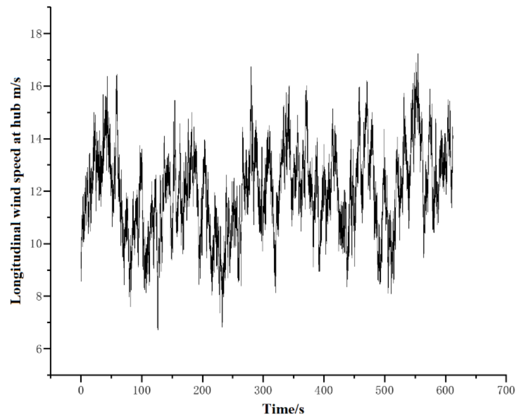

Fig. 2 Turbulent wind load spectrum at t hub (Kaimal wind spectrum)

In practical working conditions, the standard deviation of the *u* component in the Kaimal wind spectrum model undergoes certain variations due to spatial coherence influences.

(2) Spatial Coherence Model

To ensure consistency between calculation and actual conditions in establishing a three-dimensional pulsating fluid field, the wind speed distribution across the entire swept area of the wind turbine cannot be calculated using a single-point wind load spectrum alone; rather, consideration must be given to the mutual relationship between various streamlines in space, which can be expressed through a spatial coherence model. The IEC defines this relationship as the flow direction component fluid field coherence function (IEC 61400-3, 2001).

$$Coh_{i,j} = \exp\left(-a\sqrt{\left(\frac{f_r}{\bar{u}_{hub}}\right)^2 + \left(0.12\frac{r}{L_C}\right)^2}\right)$$

Where, r is the distance between any point i and j on the grid; f is the frequency; L_C is the coherent scale parameter; $\bar{u}_{hub}$ is the average wind speed at the wheel hub. The wind speed distribution in the fluid domain was calculated, as shown in Figure 3.

https://doi.org/10.5194/wes-2024-66
Preprint. Discussion started: 10 June 2024

Open Access
WIND ENERGY SCIENCE
DISCUSSIONS

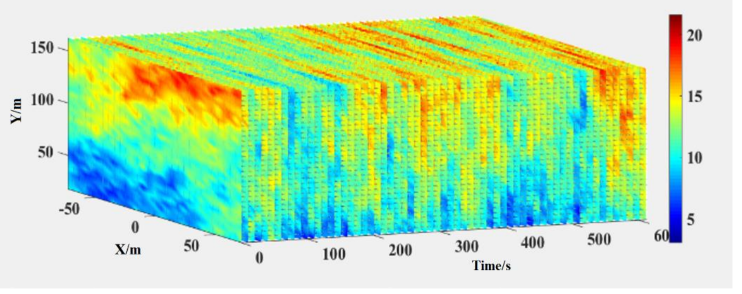

Fig. 3 Wind speed distribution in the computational fluid domain

1.2 Calculation theory of EDEM ice load

In contrast to other marine engineering structures, offshore wind turbines are characterized by their tall and flexible design. When floating ice interacts with the tower in the presence of ocean currents and when the frequency of ice loads matches the natural frequency of the overall wind turbine structure, it can lead to severe structural response. This study employs the discrete element method along with Matlock single-tooth model and asynchronous failure model to describe the interaction process between ice loads and wind turbine structures. The Matlock single-tooth numerical calculation model assumes that each ice tooth undergoes linear elastic deformation upon contact with the structure until reaching maximum deformation, after which point either no longer contacting or breaking results in zero ice force. Thus, the expression for ice force is as follows:

$$F=\begin{cases} K_{ice}\Delta_i, & 0<\Delta_i<\Delta_{\max} \\ 0, & \Delta_i\le 0, \Delta_i=\Delta_{\max} \end{cases} \tag{3}$$

Where, K_{ice} is ice tooth stiffness, N; Δ_i is the deformation of the ith ice tooth, m; Δ_{max} is the maximum deformation of ice teeth, m. The floating ice calculation domain is shown in Figure 4.

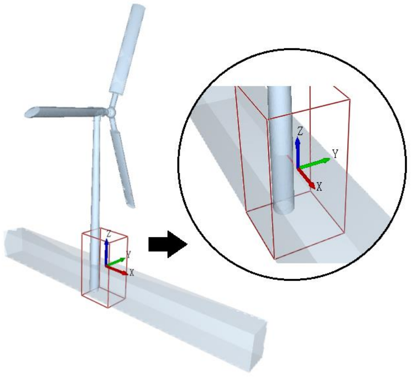

Fig. 4 Calculation domain of floating ice impact of wind turbine tower

https://doi.org/10.5194/wes-2024-66
Preprint. Discussion started: 10 June 2024

In the asynchronous failure model, the ice tooth stiffness is determined based on the uniaxial compressive strength of ice. Once the quasi-static ice force acting on the failure zone i reaches its limit, failure of the corresponding ice element occurs. The total ice load at time t can be calculated as the summation of local ice loads and can be expressed as follows:

$$F = \begin{cases} K_{ice}\left[y + V_{ice}t - L(n-1)\right], & 0 < \Delta \leq \Delta_L \\ 0, & \Delta \leq 0 \end{cases} \tag{4}$$

To enhance the precision of load calculation on wind turbine tower post floating ice impact, it is crucial to emphasize the bonding bond (i.e., connection bond) among particles while establishing an ice model. The bonding strength in the bonding bond is determined by the physical and chemical compositions of ice, ultimately determining its structural type as depicted in Figure 5.

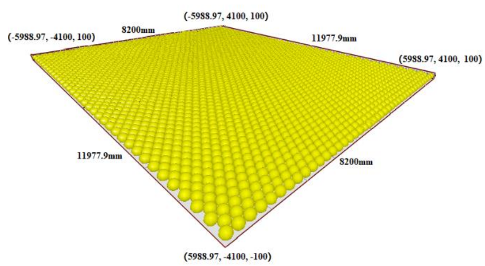

Fig. 5 Ice floe model

2 Working condition simulation

Wind turbines running in cold regions are subjected to a complex working environment, where wind load, wave load, and ice load act together on the tower of wind turbines. The schematic diagram illustrating the coupling of these loads is presented in Figure 6. In the calculation of wind load, a turbulent fluid domain is established based on the Kaimal wind speed spectrum, and the momentum-leaf element theory is employed to determine the wind load acting on offshore wind turbines.

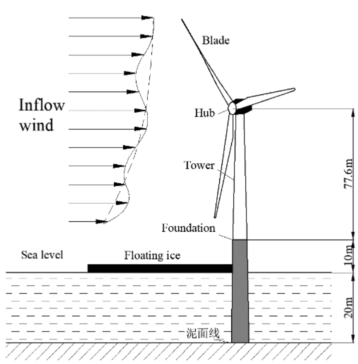

https://doi.org/10.5194/wes-2024-66
Preprint. Discussion started: 10 June 2024

Fig. 6 Schematic diagram of loading of offshore wind turbines

2.1 Turbulent fluid domain

In the natural environment, air flow exhibits spatial non-uniformity and temporal unsteadiness. To capture the statistical characteristics of wind speed time series in three directions, this study employs TurbSim, an open-source turbulent wind stochastic simulator developed by NREL. The wind speed power spectrum in the frequency domain is transformed into the time domain using inverse Fourier transform, enabling generation of three-dimensional turbulent wind data for multiple points within the flow field domain based on spatial coherence function. The structural dynamic response analysis and calculation of wind turbines are facilitated by calling the wind data file during computation. Taking the NREL 5MW wind turbine as a case study, its key structural parameters are presented in Table 1.

Tab. 1 Main parameters of NREL 5MW wind turbine

Parameter	Value	Parameter name	Value
Rated power	5MW	Cut-in wind speed	25 m/s
Tower height	87.6m	Cut-out wind speed	3 m/s
Hub height	90m	Rated wind speed	11.4m/s
Hub diameter	3m	Rotor quality	1.11×10^5kg
Rotor diameter	126m	Engine room mass	2.4×10^5kg
Control system	Synchronous pitch	Tower mass	3.48×10^5kg

In the calculation process of OpenFAST, the fluid calculation domain's coverage area encompasses the entire range of the wind turbine and tower. Therefore, the fluid calculation domain is divided into regions based on the hub point. Considering the structural size data of the wind turbine and ensuring accurate calculations for maximum tower deformation, a calculation interval within a 145m×145m range at hub center height is determined. This interval is further divided into 15 grid regions for individual calculations. The flow field calculation area's grid division can be seen in Figure 7, while maintaining the wind turbine's tower top coordinate system as the basis for calculating coordinates.

https://doi.org/10.5194/wes-2024-66
Preprint. Discussion started: 10 June 2024

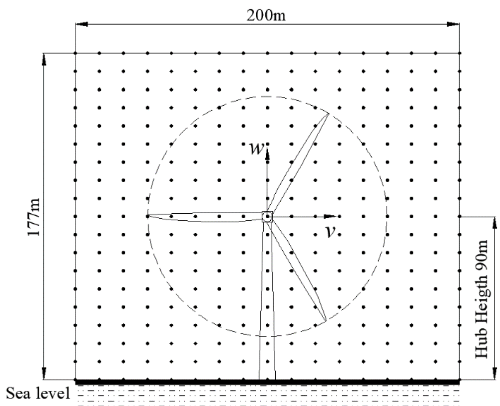

Fig. 7 Regional division of flow field

With the hub center as the reference point, based on relevant offshore wind resource data (LI Guanghua et al., 2018), the time-domain average wind speed at the reference calculation point was determined to be 12m/s, with a calculation time of 600s and a time step of 0.05s. By applying an inverse FFT transform to the NWTCUP wind spectrum model (LI Chuangdi et al., 2019) and considering spatial coherence, we obtained the wind speed variation characteristics at each grid node, which are depicted in Figure 8 showcasing the wind speed distribution within the turbulent flow field calculation domain. As illustrated in Figure 8, it is evident that the wind speed within this flow field undergoes iterative changes over time, exhibiting noticeable variations in vertical direction due to wind shear.

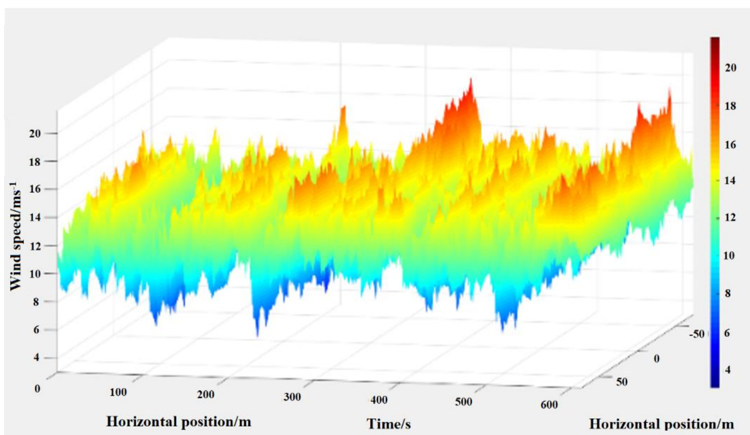

Fig. 8 Three-dimensional wind velocity distribution in the turbulent flow field calculation domain

2.2 Selection of working conditions

The effect of ice load on the tower foundation of wind turbines is primarily determined by various factors, including ice speed, ice thickness, ice drift direction, and the movement of floating ice with ocean currents.

https://doi.org/10.5194/wes-2024-66
Preprint. Discussion started: 10 June 2024

Therefore, the calculation of ice load involves considering wave load in a coupled superposition analysis. In line with the research objectives of this study, we initially assume that wind load and ice load are independent from each other. Additionally, we assume that the wind flow direction aligns with the drift direction of the ice and that the running speed of ocean currents carrying ice is a key influencing factor for failure modes related to loads. The failure modes associated with ice load can be categorized into three forms: intermittent extrusion fracture, frequency self-locking fracture, and continuous extrusion fracture failure. Typically, when the ocean velocity in an area covered by floating ice is less than or equal to $0.02 m\cdot s^{-1}$, intermittent extrusion fractures occur. When the velocity falls within ($0.02 m\cdot s^{-1}$, $0.04 m\cdot s^{-1}$), frequency self-locking extrusion fractures are observed in floating ice conditions; whereas velocities exceeding $0.04 m\cdot s^{-1}$ result in continuous extrusion fractures in floating ice scenarios. The calculation conditions for wind turbines under coupling effects between wind and ice loads are presented in Table 2.

Tab. 2 Calculation conditions of offshore wind turbines

No.	Ice load breaking type	Ice speed /$m\cdot s^{-1}$	Ice thickness /mm	Wind speed at hub height / $m\cdot s^{-1}$
1	/	/	/	12.0
2	Intermittent crushing	0.01	12.5	/
3	Frequency self-locking crushing	0.021	12.5	/
4	Continuous crushing	0.05	12.5	/
5	Intermittent crushing	0.01	12.5	12.0
6	Frequency self-locking crushing	0.021	12.5	12.0
7	Continuous crushing	0.05	12.5	12.0

According to the conditions in the northern sea area of China (HUANG Lin et al., 2013), an ice thickness of h=0.0125m was specified in the ice load boundary file. For different operational scenarios, values of $v_{ice}=0.01 ms^{-1}$, $0.021 ms^{-1}$, and $0.05 ms^{-1}$ were assigned for ice and ocean current velocities respectively. The structure diameter D was set at 4m, indentation coefficient I_{km} at 2.7, ice brittleness strength σ=5MPa, ice teeth spacing P=1m, and maximum elastic deflection Δ_{max}=1m. Figure 9 illustrates the time history curve depicting the variation in ice load under these three distinct working conditions.

https://doi.org/10.5194/wes-2024-66
Preprint. Discussion started: 10 June 2024

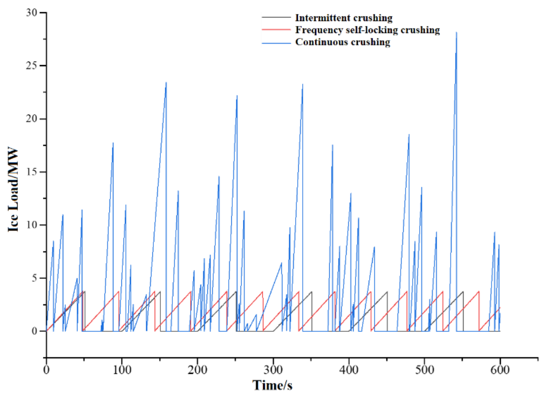

Fig. 9 The time history curve of ice loading

3 Engineering example calculation

3.1 Coupling effect of wave-ice load

This paper focuses on investigating the impact load and unit load of wind turbine towers subjected to floating ice, while analyzing the influence of different running speeds and thicknesses of floating ice on these towers. Figure 10 illustrates the occurrence of broken ice when the floating ice thickness is 12.5mm and the ice speed is respectively 0.01m/s and 0.05m/s. Table 3 presents the impact load and unit load of wind turbine towers for varying floating ice running speeds, namely, 0.01m/s, 0.021m/s, and 0.05m/s.

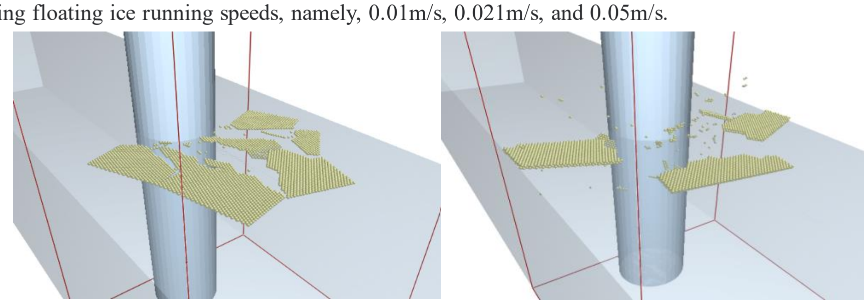

a) v_i=1.0m/s   b) v_i=5.0m/s

Fig. 10 Fragmentation of floating ice with ice thickness of 12.5mm at different flow rates

Tab. 3 Ice thickness of 12.5mm, ice of speed 0.01m/s, 0.021m/s, 0.05m/s wind turbine tower load and unit load

v_i m/s	Impact load on the tower	Unit load on the tower
0.01	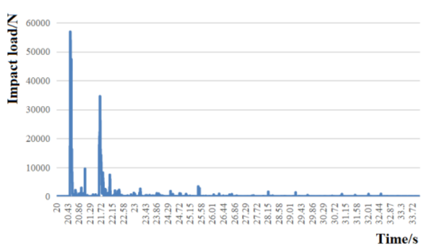	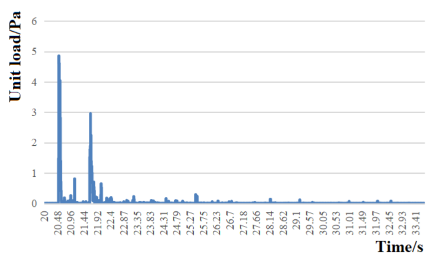

https://doi.org/10.5194/wes-2024-66
Preprint. Discussion started: 10 June 2024

0.021	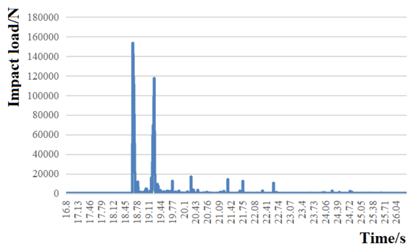	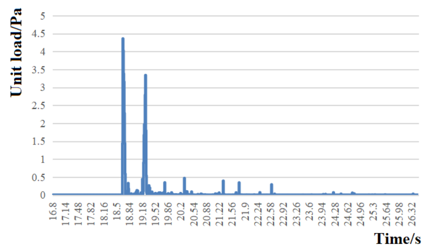
0.05	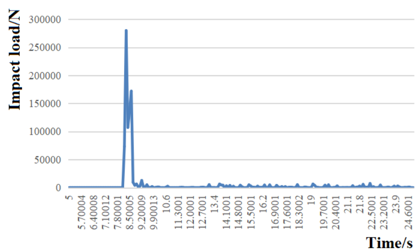	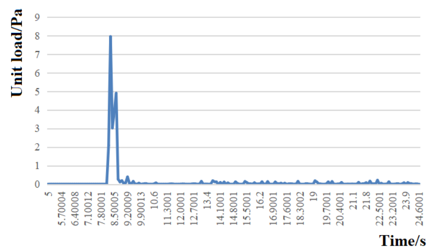

3.2 Coupling effect of wind-wave-ice load

The longitudinal displacement of the wind turbine tower top under the coupling effect of wind-wave-ice load, as shown in Fig.11a, is significantly greater than that under the coupling effect of wave-ice load alone. Moreover, the amplitude (displacement) of the tower top under the combined effect of all three loads is larger and more intense. Notably, when subjected to ice load alone, the vibration at the tower top fluctuates around its centerline with a rapid decay in amplitude from maximum to minimum after 80s. Conversely, under wind load alone or coupled with all three loads, the vibration equilibrium point at the tower top shifts approximately 0.3m along its longitudinal direction (i.e., x-direction in terms of tower top coordinate system). This indicates that when exposed to wind load, bending occurs along the flow direction and cannot be effectively recovered within this period. Additionally, when ice and wave loads are combined, there is an offset between their respective bending directions and resulting vibration equilibrium points at the tower. As depicted in Fig.11b regardless of variations in magnitude or direction for wind load conditions observed here, the vibration equilibrium point for longitudinal bending moment remains consistent with geometric shape center across different scenarios. Moreover, coupling effects among wind-wave-ice loads result in significantly greater vibrations compared to individual loading conditions. Furthermore, the shape and trend exhibited by longitudinal loading curves at foundation level remain consistent across these three working conditions, and it's worth noting that vibrational amplitude changes are considerably higher when all three loads are coupled compared to individual loading effects.

https://doi.org/10.5194/wes-2024-66
Preprint. Discussion started: 10 June 2024

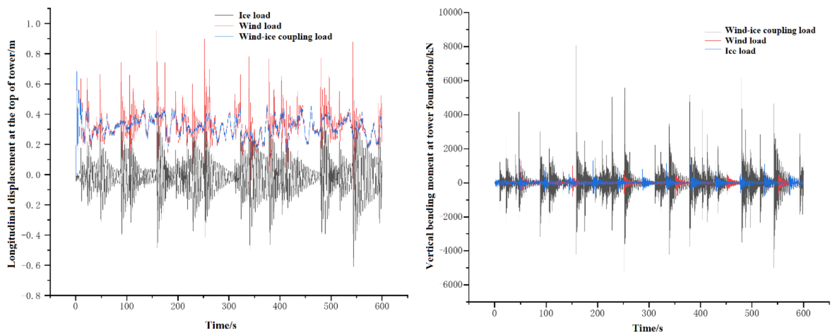

a) Amplitude b) Bending moment

Fig. 11 Longitudinal physical quantities of offshore wind turbines under load

The longitudinal load and lateral load at the tower top of the wind turbine under the three-load coupling effect are shown in Fig. 12a, while Fig. 12b illustrates the lateral bending moment and longitudinal bending moment at the tower foundation under the same effect. Since the direction of bending moment is perpendicular to that of load, i.e., transverse vector direction of tower load aligns with longitudinal vector direction of bending moment, it can be observed from Figure that both load and bending moment exhibit vibrations around the geometric center of the tower as their equilibrium point in its longitudinal direction. However, along the lateral direction, both load and bending moment experience varying degrees of displacement from their respective equilibrium points due to loads applied. Moreover, it is noteworthy that while there exists higher amplitude variation in loads longitudinally compared to laterally with more random patterns; for bending moments, higher amplitude variations occur laterally than longitudinally with greater randomness as well. Nevertheless, overall randomness degree is found to be higher for loads than for bending moments.

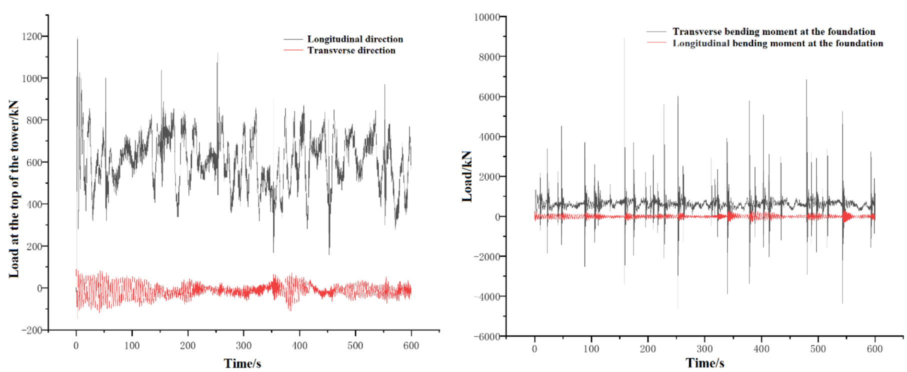

a) Top load b) Foundation load

Fig. 12 Load changes of offshore wind turbines

The lateral vibration amplitude of the support platform of wind turbines is generally greater than the longitudinal vibration amplitude under various working conditions, as depicted in Figure 13. Moreover, the

https://doi.org/10.5194/wes-2024-66
Preprint. Discussion started: 10 June 2024

longitudinal vibration amplitude remains small and exhibits overall stability, while the lateral vibration displacement shows significant variability. Considering the impact of individual wind loads or ice loads, it is observed that ice load has a higher effect compared to wind load. Furthermore, when considering coupling loads, their effect surpasses that of any single load in terms of both tower amplitude after ice load and tower amplitude attenuation frequency.

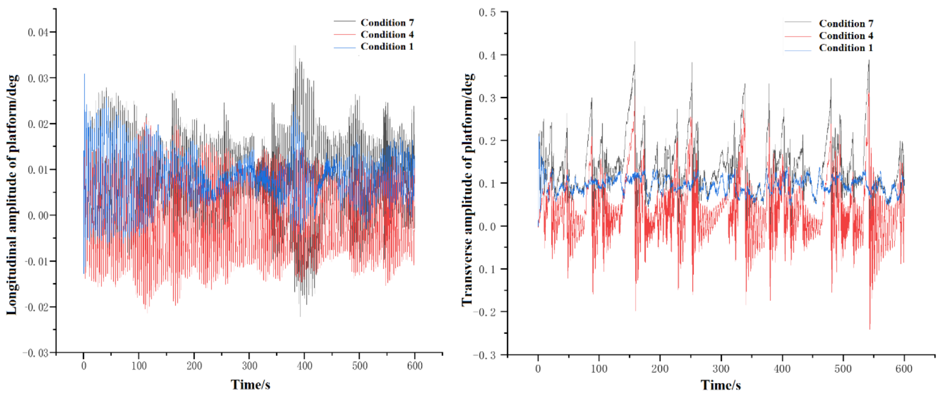

a) Longitudinal amplitude b) Transverse amplitude

Fig.13 Amplitude of offshore wind turbine platform under load

The findings in Figure 14 demonstrate that, regardless of the running conditions of offshore wind turbines, the vibration pattern and trend of the tower support platform align with those observed for tower vibration displacement. Moreover, both in terms of amplitude and frequency, lateral load vibrations surpass longitudinal vibrations.

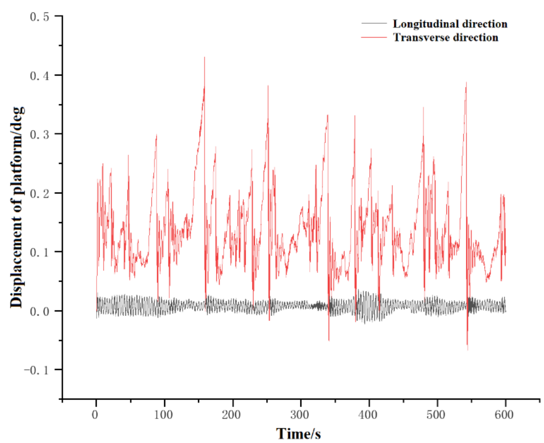

Fig. 14 Comprehensive vibration displacement changes of the platform under load

3.3 Fatigue damage estimation

https://doi.org/10.5194/wes-2024-66
Preprint. Discussion started: 10 June 2024

The fatigue damage of wind turbines under the single action of wind load, ice load, and the coupling effect of wind-wave-ice three loads is calculated in the time domain to analyze their long-term effects on load accumulation. This study compares and analyzes the fatigue damage of offshore wind turbines under these three working conditions using both the quadratic superposition method and DNV method for damage combination calculation. As shown in Table 4, regardless of whether the quadratic superposition method or DNV method is used for analysis and calculation, it is evident that the fatigue damage caused by ice load alone is lower than that caused by wind load alone, while the fatigue damage under coupling loads is lower than that under single loads. During wind-wave-ice coupling, results from the quadratic superposition method yield smaller calculations compared to those from DNV's superposition method which yields larger but more accurate results suitable for engineering applications in assessing fatigue damage of offshore wind turbines.

Tab.4 Fatigue damage of offshore wind turbines under different working conditions and different algorithms

Wind load	Ice load	Load coupling	Quadratic superposition method	DNV method
7.43×10^{-8}	5.23×10^{-8}	4.11×10^{-8}	9.12×10^{-8}	5.02×10^{-7}

4 Conclusion

The present study investigates the dynamic response of offshore wind turbines subjected to wind load, wave load, ice load, and their coupled effects. Additionally, an estimation of fatigue damage is conducted. The obtained results demonstrate that:

(1) Under the separate action of wind load and ice load, the horizontal and longitudinal bending moments at the tower foundation of wind turbines are essentially identical. When wind-wave-ice load is coupled, the horizontal and longitudinal bending moments at the tower foundation of wind turbines exceed those under individual loads. Additionally, due to wind load participation, the equilibrium point for tower vibration in wind turbines shifts along the direction of the wind load vector, with a linear translation corresponding to the calculated wind speed. Under isolated ice load conditions, both horizontal and longitudinal amplitudes at the top of wind turbines are smaller compared to those under isolated wind load conditions. This can be attributed to a longer duration of action for wind loads despite their lower instantaneous impact force when compared to ice loads; thus resulting in more pronounced cumulative effects. When considering coupled wind-wave-ice loading scenarios, although similar trends are observed as seen under individual actions from winds and ice alone, there exist significant differences in amplitude and attenuation rate. The displacement offset experienced by support platforms in response to combined loading is greater than that caused by either winds or ice alone; moreover, lateral displacement significantly exceeds longitudinal displacement on these platforms. Furthermore, it should be noted that compared with its influence on tower foundations from winds alone, ice loads have a more noticeable effect on displacements.

(2) When analyzing the impact of ice load on standalone wind turbines, the discrete element method is employed to investigate the characteristics of floating ice impacting offshore wind turbine towers. To enhance the

accuracy in calculating the tower's impact load caused by ice, the mutual influence resulting from changes in floating ice composition is achieved through designing numerical values for bonding bonds between particles. This approach helps narrow the gap between simulation calculations and actual working conditions. The analysis and calculation results reveal that the velocity at which floating ice moves significantly affects wind turbine towers. Therefore, in practical projects, a well-designed tower foundation platform structure can be implemented to reduce the speed at which floating ice moves, thereby mitigating damage caused by both floating ice and other objects to supporting platforms of wind turbines while enhancing their structural stability and reliability.

(3) The fatigue damage value of wind load and ice load on wind turbines under separate action is greater than the effect of coupling load, as the direction and magnitude of wind load are uncertain. This uncertainty helps to balance the fatigue damage caused by ice load and wave load on wind turbines to some extent. In the calculation process, the DNV method yields a higher damage value through superposition calculation compared to the calculation result considering load coupling effects. From an engineering design and evaluation perspective, this indicates a higher safety factor for the DNV method. Therefore, it is recommended to utilize the DNV method in practical engineering applications for evaluating the fatigue life of offshore wind turbines under coupling loads.

Competing interests： The contact author has declared that none of the authors has any competing interests.

Reference

[1] LIU Weimin, LIU Lei, Chen Fengyun et al. Progress of Marine renewable energy technology in China [J]. Science and Technology Review, 2019, 38 (14) : 27-39. (in Chinese)
[2] ZHANG Dayong, WANG Guojun, WANG Shuaifei et al. Analysis of ice resistance of offshore wind power foundation in ice region [J]. Journal of Ship Mechanics, 2018,175 (5) : 101-113. (in Chinese)
[3] HUANG Yan, MA Yuxian, LUO Jinping et al. Analysis of ice-induced vibration of single-column three-pile offshore wind power structure in Bohai Sea [J]. Ocean Engineering, 2016,34 (05) : 1-10. (in Chinese)
[4] SHI Wei, XUE Ruining, HOU Xiaobin et al. Dynamic response of 10 MW class semi-submersible floating fan [J], Marine Engineering, 2021,43 (10) : 1-9+43. (in Chinese)
[5] HU Xuan, YE Kehua, LI Chun et al. Mechanical response analysis of wind power under asynchronous ice load [J], Thermal Energy and Power Engineering, 2019, 36 (02) : 123-131. (in Chinese)
[6] YANG Dongbao, GAO Junsong, LIU Jianping et al. Ice-induced vibration analysis of offshore fan structure based on DEM-FEM coupling method [J], Chinese Journal of Mechanical Mechanics, 201, 53 (03) : 682-692. (in Chinese)
[7] WANG Guojun, WANG Shuaifei, SONG Chu et al. Research on cone ice load of wind power foundation based on measured data [J], Journal of Ship Mechanics, 2022,26 (03) : 375-382. (in Chinese)
[8] HUANG Yan, MA Yuxian, LUO Jinping et al. Analysis of ice-induced vibration of single-column three-pile offshore wind power structure in Bohai Sea [J]. Ocean Engineering, 2016,34 (05) : 1-10.
[9] ZHANG Lixian, SHI Wei, LI Xin et al. Dynamic characteristics of large single-pile offshore wind turbine under combined wind and ice action [J]. Acta Solar Energy Sinica, 2019, 44 (02) : 59-66. (in Chinese)
[10] BA Yueqiao. Ice fatigue Analysis of stationary offshore wind turbine structure in Ice region [D]. Dalian University of Technology, 2019. (in Chinese)
[11] LIU Hualiang. Research on testing method of filling capacity of freshly mixed self-compacting concrete [D]. University of South China, 2008.
[12] Wang Q. Ice-inducted vibrations under continuous brittle crushing for an offshore wind turbine[D]. Norwegian University of Science and Technology,2015.
[13] Wei Shi,Xiang Tan,Zhen Gao,Torgeir Moan. Numerical study of ice-induced loads and responses of a monopile-type offshore wind turbine in parked and operating conditions[J]. Cold Regions Science and Technology,2016,123:121-139

https://doi.org/10.5194/wes-2024-66
Preprint. Discussion started: 10 June 2024

[14] Matlock Hudson,Dawkins William P.,Panak John J. . Analytical Model for Ice-Structure Interaction[J]. Journal of the Engineering Mechanics Division,1971,97(4).

[15]T. Kärnä,K. Kamesaki,H. Tsukuda. A numerical model for dynamic ice – structure interaction[J]. Computers and Structures,1999,72(4).

[16] VERITAS D N. DNV-RP-C205,Environmental conditions and environmental loads[S]. Oslo,2010.

[17] International Electrical Commission. IEC 61400-1,Wind turbines–Part 1:Wind turbines[S]. London, 2005.

[18] International Electrical Commission. IEC 61400-3,Wind turbines–Part 3:Design requirements for offshore wind turbines [S]. London,2001.

[19] LI Guanghua, ZHOU Jinna, XU Chang et al. Research on fine power output modeling of offshore wind farm considering wind resource characteristics [J], Renewable Energy, 2018,36 (05) : 778-784. (in Chinese)

[20] LI Chuangdi, Li Yuxiang, YANG Xuefeng et al. Complex mode method for six-parameter practical viscoelastic damping structures based on Davenport wind spectrum for wind vibration response [J]. Applied Mathematics and Mechanics, 2019, 44 (03) : 248-259. (in Chinese)

[21] HUANG Lin, SUN Jia, YANG Yiqiu et al. The relationship between sea surface height (SSH) and wind stress in the North Pacific Ocean [J], Oceanologia et Limnologia Sinica, 2013,44 (01) : 111-119. (in Chinese)